



# The microstructure and magnetic susceptibilities of $\text{LaFe}_{11.4}\text{Si}_{1.6}$ compound

J.D. Zou<sup>a,b,\*</sup>, W. Li<sup>b</sup>, B.G. Shen<sup>c</sup>, J.R. Sun<sup>c</sup>

<sup>a</sup> School of Materials Science and Engineering, Beihang University, Beijing 100191, China

<sup>b</sup> Division of Functional Materials, Central Iron and Steel Research Institute, Beijing 100081, China

<sup>c</sup> State Key Laboratory for Magnetism, Institute of Physics, Chinese Academy of Sciences, Beijing 100190, China

## ARTICLE INFO

### Article history:

Received 17 March 2010

Received in revised form 16 July 2010

Accepted 20 July 2010

Available online 4 August 2010

### Keywords:

Magnetic susceptibility

Magnetic properties

Electron diffraction

Magnetic intermetallics

## ABSTRACT

The fabrication processes of bulk  $\text{LaFe}_{13-x}\text{Si}_x$  compounds are usually time-consuming but significantly impact on the microstructural and magnetic properties. High-resolution transmission electron microscope (HRTEM) and bulk magnetometry measurements are employed to study the microstructural and magnetic properties of  $\text{LaFe}_{11.4}\text{Si}_{1.6}$  compound. The crystallization status frozen by quenching is uncovered completely through the HRTEM observations. Besides of crystalline structure, both noncrystalline and nanocrystalline structures are observed. This behavior may originate from the difficulty in the combining capacity between Fe and La. The magnetic measurements reveal that dc and ac inversed susceptibilities are not consistent under strong and weak applied magnetic fields. The behaviors of magnetic susceptibilities deviate from the Curie–Weiss law under weak applied magnetic fields.

© 2010 Elsevier B.V. All rights reserved.

## 1. Introduction

Pursue materials showing large magnetocaloric effect (MCE) are very important for development magnetic cooling devices and have attracted increasing attentions [1–4]. Many efforts have been made to improve the performance of magnetocaloric materials. However, a number of factors determine the MCE, and need to be investigated deeply. Recently, some researchers start to study the microstructural properties and their influences on the MCE [5–7], but so far the researches in this area are still very limited. The  $\text{NaZn}_{13}$ -type  $\text{LaFe}_{13-x}\text{Si}_x$  compounds are employed to investigate the relationship between the microstructural and magnetic properties. The  $\text{LaFe}_{13-x}\text{Si}_x$  compounds have been intensively studied owing to large magnetocaloric effect (MCE) (Ref. [8–12]), large spontaneous magnetovolume effect [8,9,13–16], and itinerant electron metamagnetic (IEM) transition (Ref. [13–17]) etc.  $\text{LaFe}_{13-x}\text{Si}_x$  compounds are looked as proposing magnetic refrigerant. Interestingly, the  $\text{LaFe}_{13}$  compound cannot be obtained directly because of positive formation enthalpy between lanthanum and iron. Usually, substitutions of some Si or Al for Fe are employed to stabilize the bulk  $\text{NaZn}_{13}$ -type  $\text{LaFe}_{13-x}\text{Si}_x$  compounds (space group  $Fm\bar{3}c$ ), while time-consuming annealing and quenching are required. Nevertheless, the quenched  $\text{LaFe}_{13-x}\text{Si}_x$  compounds are metastable. It is imaginable that the crystallization processes will have great

influence on the properties of the quenched samples. The following discussions will reveal the correlations between the crystallization processes and the magnetic properties.

The cubic  $\text{LaFe}_{13-x}\text{Si}_x$  compounds can be stabilized in the composition range between  $x = 1.56$  and  $2.47$  [18]. The samples with low silicon concentration can be synthesized by extending heat treatment time. The first-order phase transition between the ferromagnetic (FM) and paramagnetic (PM) state occurs at Curie temperature. Many efforts have been made to explore the influence of applied magnetic field, interstitial atom, and pressure etc on the properties of  $\text{LaFe}_{13-x}\text{Si}_x$  compounds [13–17,19], whereas the importance of microstructure is not totally realized. The microstructural information is helpful to understand the properties of quenched  $\text{LaFe}_{13-x}\text{Si}_x$  compounds [7]. Here the crystallization processes of  $\text{LaFe}_{11.4}\text{Si}_{1.6}$  are analyzed by HRTEM. The magnetic properties impacted by the crystallization processes will be investigated by the bulk magnetometry study.

## 2. Experimental details

Stoichiometric  $\text{LaFe}_{11.4}\text{Si}_{1.6}$  sample with the normal compositions was prepared by arc melting the pure materials under ultra-pure argon gas atmosphere in a water-cooled copper crucible. The product was sealed in a quartz tube of high vacuum, and then annealed at 1343 K for 58 days. Subsequently, the sample was quenched in liquid nitrogen. The specimen with the  $\text{NaZn}_{13}$ -type structure was confirmed by the X-ray powder diffraction (XRD) study at room temperature. HRTEM analysis with conventional powder sample was carried out on a JEM 2010 TEM with a 200 kV accelerating voltage. The dc and ac magnetization measurements were performed using physical properties measurement system (PPMS) from Quantum Design Inc. Temperature dependence of magnetization was measured on heating. The zero-field-cooling (ZFC) and fixed point model were adopted. The oscillate mode is used to reduce residual field (from 2 T to 0 T).

\* Corresponding author at: School of Materials Science and Engineering, Beihang University, XueYuan Road No.37, Beijing 100191, China. Tel.: +86 10 82317132, fax: +86 10 82317133.

E-mail addresses: [zoujd@buaa.edu.cn](mailto:zoujd@buaa.edu.cn), [zoujd@yahoo.com.cn](mailto:zoujd@yahoo.com.cn) (J.D. Zou).

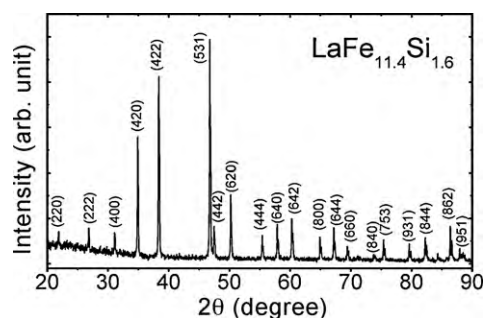


**Fig. 1.** Room temperature XRD pattern of  $\text{LaFe}_{11.4}\text{Si}_{1.6}$ . The diffraction peaks are indexed.

### 3. Experimental results and discussion

#### 3.1. HRTEM analysis

The XRD pattern of  $\text{LaFe}_{11.4}\text{Si}_{1.6}$  is shown in Fig. 1 confirming the  $\text{NaZn}_{13}$ -type structure. The lattice constant extracted from XRD pattern is 11.4654 Å. The bright field image of  $\text{LaFe}_{11.4}\text{Si}_{1.6}$  is shown in Fig. 2(a). A corresponding dark field image is shown in Fig. 2(b). Comparing with the bright field image, it should be noted that some nanocrystals (from several nanometers to tens of nanometers) are observed. The bright spots in the dark field image convincingly indicate the grain sizes and shapes of the nanocrystals. HRTEM image are shown in Fig. 3. The nanocrystals are surrounded by dash lines approximately. The dash lines clearly depict the grain sizes, grain boundary features, and grain shapes of the nanocrystals. The non-crystalline areas are observed together with the nanocrystals. The nano-scale grains embed in the noncrystalline area and look like islands. Despite this, the micron-scale crystalline grains are majority in the heat-treated bulk  $\text{LaFe}_{11.4}\text{Si}_{1.6}$  compound. The HRTEM images portray the features of crystallization status at high temperature frozen by quenching.

In fact, the cooling rates of liquid nitrogen quenching are not sufficient to produce metallic noncrystalline structure. Usually, noncrystalline alloys are produced by rapid solidification from the melt, and cooling rates of order  $10^5$  C/s are generally required [20]. It is possible that the slow crystallization processes lead to the emergence of noncrystalline structures in bulk  $\text{LaFe}_{13-x}\text{Si}_x$  compounds. That is in a sense the reason for the metastability of  $\text{LaFe}_{13-x}\text{Si}_x$  compounds. The long-term heat treatment promotes the atom diffusion, and homogenizes the alloy which is favorable for the formation of  $\text{NaZn}_{13}$ -type structure. Due to the intrinsic

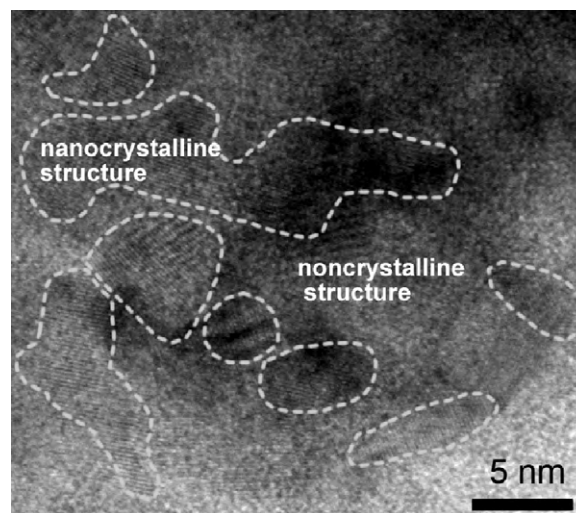


**Fig. 3.** Room temperature HRTEM image of  $\text{LaFe}_{11.4}\text{Si}_{1.6}$ . Nanocrystals are surrounded by dash lines approximately.

difficulty in combining capacity, however, some atoms form nano-scale grains, and some atoms even form noncrystalline structure. Therefore, some of crystallization processes cannot be entirely finished and frozen by liquid nitrogen quenching.

#### 3.2. dc bulk magnetometry measurements results

The bulk magnetometry studies were performed on the synthesized products in order to reveal the influence of the crystallization process. Temperature dependences of dc magnetizations are shown in Fig. 4(a) and (b). With the increase in applied magnetic field, Curie temperatures move up (from 198 K at 20 mT to 218 K at 5 T) which present the typical feature of first-order phase transition. Curie temperatures are determined by the extremum of first derivative of  $M$ - $T$  curves. Temperature dependence inversed magnetic susceptibilities under various applied fields are shown in Fig. 4(c) and (d), respectively. The data under strong applied fields (above 0.2 T) present good consistency. The  $\chi^{-1}$ - $T$  relation, however, deviates from each other under weak applied fields (below 40 mT), and are not consistent with those under strong applied field (above 0.2 T). This result is in contrast to native expectations based on the Curie–Weiss law that inversed susceptibilities should be unanimous in their paramagnetic states, whether the applied

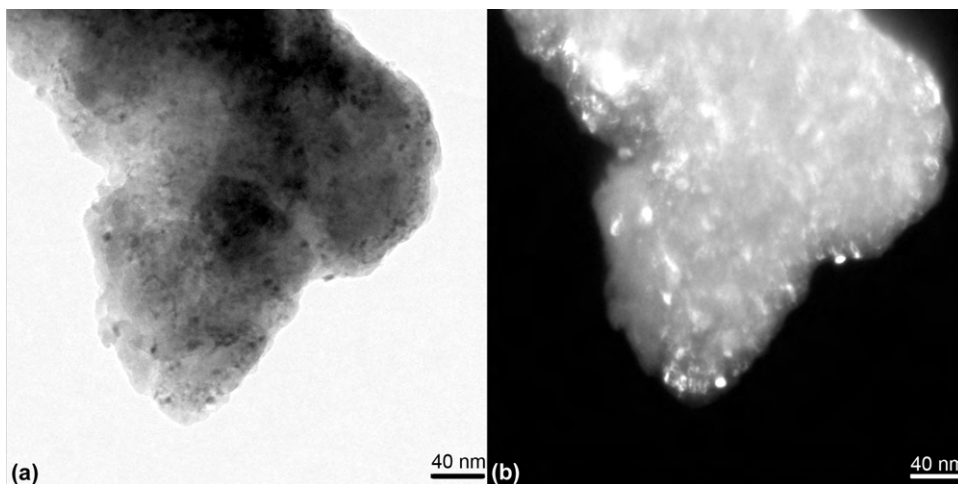


**Fig. 2.** (a) The bright field image of  $\text{LaFe}_{11.4}\text{Si}_{1.6}$ . (b) The corresponding dark field image of  $\text{LaFe}_{11.4}\text{Si}_{1.6}$ .

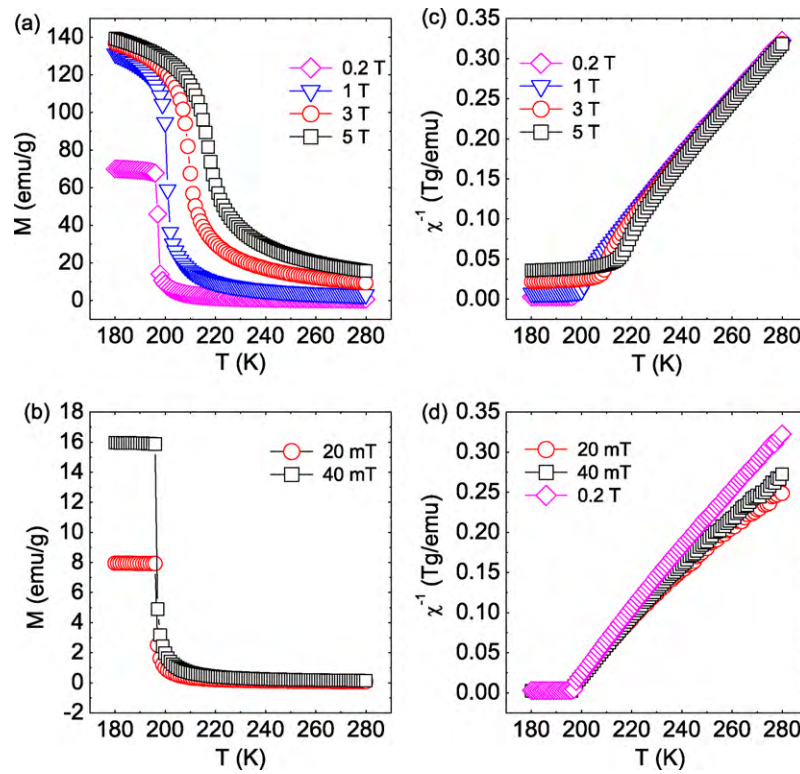


**Fig. 4.** The dc magnetizations of  $\text{LaFe}_{11.4}\text{Si}_{1.6}$ . (a) and (b) Temperature dependences of magnetizations measured on heating from 180 K to 280 K under different applied field after zero-field-cooling. (c) and (d) The dc inverse susceptibilities. The  $\chi^{-1}$ - $T$  relations above  $T_C$  consist with the Curie–Weiss law above 0.2 T, but depart from Curie–Weiss law lower than 40 mT.

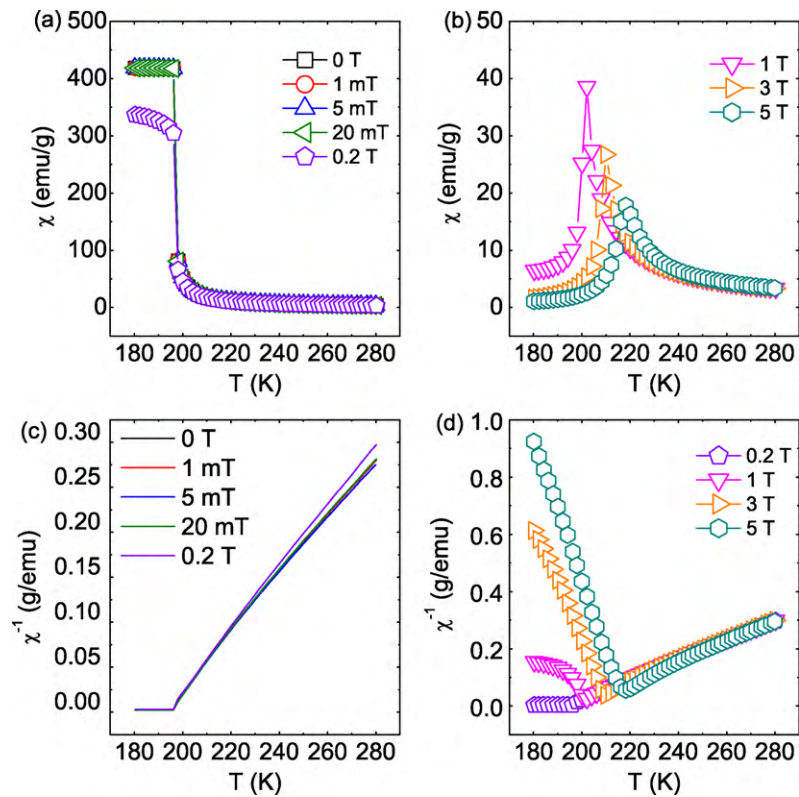


**Fig. 5.** The ac magnetic susceptibilities of  $\text{LaFe}_{11.4}\text{Si}_{1.6}$ . (a) and (b) Temperature dependences of ac magnetic susceptibilities measured on heating from 180 K to 280 K under different applied field after zero-field-cooling. (c) and (d) Temperature dependences of ac inverse susceptibilities. The amplitude of ac field is 10 Oe, and the frequency is 1000 Hz.



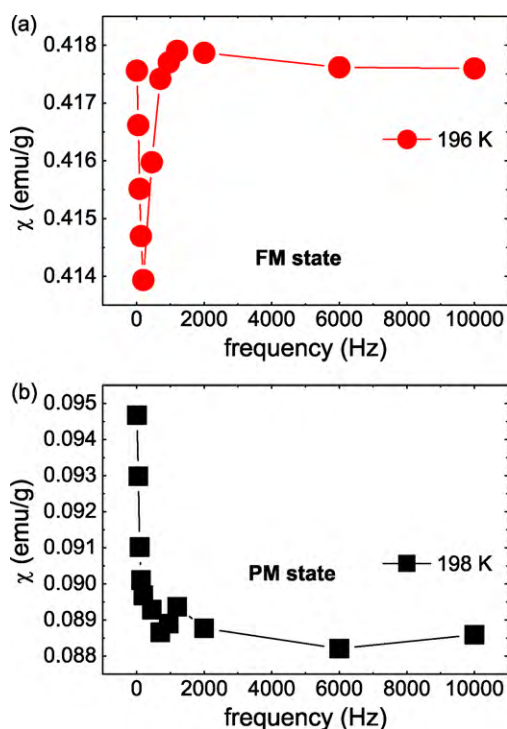


**Fig. 6.** The frequency dependences of ac susceptibilities of LaFe<sub>11.4</sub>Si<sub>1.6</sub>. (a) The ac susceptibilities below  $T_C$  (at 196 K). (b) The ac susceptibilities at  $T_C$  (at 198 K). The amplitude of ac field is 10 Oe, and the dc field is zero.

field strong or weak. The similar behaviors are previously observed in the LaFe<sub>11.5</sub>Si<sub>1.5</sub> sample [7].

### 3.3. ac bulk magnetometry measurements results

In order to verify the anomalous susceptibilities, the ac magnetic measurements are employed. Fig. 5(a) and (b) shows the temperature dependence of ac susceptibilities, Fig. 5(c) and (d) shows the temperature dependence of inversed susceptibilities. The inversed ac susceptibilities curves dovetail nicely with each other above  $T_C$  when the dc magnetic fields are lower than 20 mT or higher than 0.2 T. However, obvious discrepancies in the  $\chi^{-1}$ – $T$  relations between strong and weak applied fields conditions are observed. According to Curie–Weiss law, inversed susceptibilities should be unanimous in paramagnetic states. Fig. 6 shows the frequency dependence of ac susceptibilities. The sharp peak of FM component in the range of low frequency at 196 K is shown in Fig. 6(a). The peak disappears and the magnitude of signals seriously damped at  $T_C$  (198 K), shown in Fig. 6(b). It indicates that the possibility of FM component above  $T_C$  is excluded.

We propose that the anomalous susceptibilities may originate from the existence of noncrystalline and nanocrystalline structure. LaFe<sub>13–x</sub>Si<sub>x</sub> compounds are itinerant electron ferromagnets which may be sensitive to the atoms disorder and the finite-size of the grains. However, it is difficult to know the magnetism of noncrystalline structure completely by now. Chiang et al. [21] have revealed that the saturation magnetization of amorphous La(Fe<sub>x</sub>Al<sub>1–x</sub>)<sub>13</sub> are larger than those crystalline alloys, which support our analyses. Besides, we should pay attentions to the appearance of nanocrystal verified by the HRTEM measurements. The previous reports have shown that the finite-size effect influence the magnetic properties, especially for itinerant electron ferromagnet, such as magnetic momentum etc [22–24]. These may lead to the total angular momentum increase when the sizes of the grains decrease continuously. As results, the  $\chi^{-1}$ – $T$  relations will deviate downward

from the Curie–Weiss law.

## 4. Conclusions

HRTEM combined with ac and dc magnetic measurements are employed to study the unique properties of quenched bulk LaFe<sub>11.4</sub>Si<sub>1.6</sub> compound. Both noncrystalline and nanocrystalline structure are observed together with the micron-scale structure. These indicate that the crystallization processes cannot be entirely finished due to the poor combining capacity between Fe and La, even though the sample underwent long-term heat treatment. The magnetic properties of the synthesized sample are investigated carefully. The dc and ac bulk magnetometry measurements show that the  $\chi^{-1}$ – $T$  relations in paramagnetic states are inconsistent under strong and weak applied fields. The inversed susceptibilities under weak dc applied field dramatically depart from the Curie–Weiss law. According to the ac magnetic measurements, the influence of FM component above  $T_C$  is excluded. Therefore, the reason of anomalous susceptibilities may be ascribed to the imperfect crystalline processes. The noncrystalline and nanocrystalline structure may have different magnetic properties from the crystalline structure. As results, the susceptibilities show discrepant behaviors under strong and weak applied magnetic fields, and deviate from Curie–Weiss law. The results are benefit to understand the properties of bulk LaFe<sub>13–x</sub>Si<sub>x</sub> compounds, and promote their performance in the practical applications.

## Acknowledgments

This work has been supported by the National Natural Science Foundation of China (Grant No. 50801015, and 50921003), and the Fundamental Research Funds for the Central Universities (Grant No. YWF-10-01-1301).

## References

- [1] L. Mañosa, D. González-Alonso, A. Planes, E. Bonnot, M. Barrio, J.-L. Tamarit, S. Aksoy, M. Acet, Nat. Mater. 9 (2010) 478.
- [2] G. Tian, H.L. Du, Y. Zhang, Y.H. Xia, C.S. Wang, J.Z. Han, S.Q. Liu, J.B. Yang, J. Alloys Compd. 496 (2010) 517.
- [3] G.H. Meng, O. Tegus, W.G. Zhang, L. Song, J.H. Huang, J. Alloys Compd. 497 (2010) 14.
- [4] M. Rosca, M. Balli, D. Fruchart, D. Gignoux, E.K. Hlil, S. Miraglia, B. Ouladdiaf, P. Wolfers, J. Alloys Compd. 490 (2010) 50.
- [5] B. Podmiljsak, I. Škulj, B. Markoli, K. Žužek Rožman, P.J. McGuinness, S. Kobe, J. Magn. Magn. Mater. 321 (2009) 300.
- [6] L.S. Chumbley, O. Ugurlu, R.W. McCallum, K.W. Dennis, Y. Mudryk, K.A. Gschneidner Jr., V.K. Pecharsky, Acta Mater. 56 (2008) 527.
- [7] J.D. Zou, W. Li, B.G. Shen, Chin. Phys. B 18 (2009) 4366.
- [8] F.X. Hu, B.G. Shen, J.R. Sun, Z.H. Cheng, G.H. Rao, X.X. Zhang, Appl. Phys. Lett. 78 (2001) 3675–3677.
- [9] F.X. Hu, B.G. Shen, J.R. Sun, G.J. Wang, Z.H. Cheng, Appl. Phys. Lett. 80 (2002) 826–828.
- [10] A. Fujita, S. Fujieda, Y. Hasegawa, K. Fukamichi, Phys. Rev. B 67 (2003) 104416.
- [11] J.D. Zou, B.G. Shen, J.R. Sun, J. Phys.: Condens. Matter 19 (2007) 196220.
- [12] J.D. Zou, B.G. Shen, B. Gao, J. Shen, J.R. Sun, Adv. Mater. 21 (2009) 693.
- [13] A. Fujita, Y. Akamatsu, K. Fukamichi, J. Appl. Phys. 85 (1999) 4756–4758.
- [14] A. Fujita, S. Fujieda, K. Fukamichi, H. Mitamura, T. Goto, Phys. Rev. B 65 (2001) 014410.
- [15] A. Fujita, K. Fukamichi, M. Yamada, T. Goto, J. Appl. Phys. 93 (2003) 7263–7265.
- [16] A. Fujita, K. Fukamichi, J.T. Wang, Y. Kawazoe, Phys. Rev. B 68 (2003) 104431.
- [17] S. Fujieda, A. Fujita, K. Fukamichi, Y. Yamazaki, Y. Lijima, Appl. Phys. Lett. 79 (2001) 653–655.
- [18] T.T.M. Palstra, J.A. Mydosh, G.J. Nieuwenhuys, A.M. van der Kraan, K.H.J. Buschow, J. Magn. Magn. Mater. 36 (1983) 290–296.
- [19] A. Fujita, K. Fukamichi, M. Yamada, T. Goto, Phys. Rev. B 73 (2006) 104420.
- [20] R.C. O'Handley, Modern Magnetic Materials: Principles and Applications, John Wiley & Sons, Inc., New York, 2000.
- [21] T.H. Chiang, K. Fukamichi, T. Goto, J. Phys.: Condens. Matter 4 (1992) 7489.
- [22] P.V. Hendriksen, S. Linderoth, P.-A. Lindgard, Phys. Rev. B 48 (1993) 7259–7273.
- [23] I.M.L. Billas, J.A. Becher, A. Chatelain, W.A. de Heer, Phys. Rev. Lett. 71 (1993) 4067–4070.
- [24] I.M.L. Billas, A. Chatelain, W.A. de Heer, Science 265 (1994) 1682–1684.